

and the Y---Cu separation is about 6.3 Å. There are no hydrogen bonds between neighboring ribbons. Addition of Cu(acac)<sub>2</sub> to the benzene solution of Y(hfa)<sub>3</sub>(H<sub>2</sub>O)<sub>2</sub> yields the 1 : 1 adduct of [Y(hfa)<sub>3</sub>(H<sub>2</sub>O)<sub>2</sub>][Cu(acac)<sub>2</sub>] connected through intermolecular hydrogen bondings. This adduct dissociates to the each component by adding polar solvents. The crystal structure shows that [Y(hfa)<sub>3</sub>(H<sub>2</sub>O)<sub>2</sub>][Cu(acac)<sub>2</sub>] molecules have one-dimensional networks by intermolecular hydrogen bondings. Further studies on the control of 1 : 2 or 1 : 3 ratio of Cu to Y metal complex through intermolecular interactions are in progress in our laboratory.

**Acknowledgment.** Financial support of Korea Ministry of Education (1997-1998) is gratefully acknowledged.

### References

1. Rao, C. N. R.; Raveau, B. *Acc. Chem. Res.* 1989, 22, 6.
2. Cowley, A. H.; Jones, R. A. *Angew. Chem., Int. Ed. Engl.* 1989, 28, 1208.
3. (a) Wang, S.; Smith, K. D. L.; Pang, Z.; Wagner, M. J. *J. Chem. Soc., Chem. Commun* 1992, 1595. (b) Wang, S.; Pang, Z.; Smith, K. D. L.; Wagner, M. J. *J. Chem. Soc., Dalton Trans.* 1994, 955. (c) Bidell, W.; Shklover, V.; Berke, H. *Inorg. Chem.* 1992, 31, 5561. (d) Vaartsra, B. A.; Huffman, J. C.; Streib, W. E.; Caulton, K. G. *J. Chem. Soc., Chem. Commun* 1990, 1990.
4. Bidell, W.; Bosch, H. W.; Veghini, D.; Hund, H.-U.; Doring, J.; Berke, H. *Helvetica Chim. Acta* 1993, 76, 596.
5. Abbreviations used in this paper include: Hhfa, hexafluoroacetylacetone; hfa, anion of Hhfa; Hacac, acetylacetone or 2,4-pentanedione; acac, anion of Hacac.
6. North, A. C. T.; Phillips, D. C.; Mathews, F. S. *Acta Crystallogr., Sect A: Cryst. Phys., Diffr., Theor. Gen. Crystallogr.* 1968, 24, 351.
7. (a) Sheldrick, G. M. in *SHELXS-86*, A Program for Structure Determination, University of Gottingen, Germany, 1986. (b) Sheldrick, G. M. in *SHELXL-93*, A Program for Structure Refinement, University of Gottingen, Germany, 1993.
8. (a) Kang, S.-J.; Jung, Y. S.; Sohn, Y. S. *Bull. Korean Chem. Soc.* 1997, 18, 266. (b) Jung, Y. S.; Lee, J. H.; Sohn, Y. S.; Kang, S.-J. *Bull. Korean Chem. Soc.* 1998, 19, 15.
9. Pinkas, J.; Huffman, J.; Bollinger, J. C.; Streib, W. E.; Baxter, D. V.; Chisholm, M. H.; Caulton, K. G. *Inorg. Chem.* 1997, 36, 2930.

## Synthesis of Barium Titanyl Oxalate by Homogeneous Precipitation from Dimethyl Oxalate Solution

Myounghee Lim, Wooyoung Huh, and Chul Lee\*

Research Institute for Natural Sciences and Department of Chemistry, Hanyang University, Seoul 133-791, Korea  
Received February 14, 1998

Barium titanate (BT) is considered an attractive material as its ceramics are widely used in electronic components such as multilayer capacitors and nonlinear resistors.<sup>1,2</sup> In order to produce high-quality ceramics, the starting powders require to have a uniform particle size and shape.<sup>3</sup> Similarly, the powder of barium titanyl oxalate (BTO), known as the precursor of BT, need to have a uniform particle size and shape. In order to obtain BTO powder with such a high quality, a homogeneous precipitation method has been adopted.

A common way of homogeneous precipitation methods are the controlled release of precipitants by another chemical source in the solution. Diethyl oxalate (DEO), which can slowly decompose to yield oxalate ions, had been used as the precipitant source by present authors<sup>4,5</sup> and was found to produce BTO particles of spherical shape with a narrow size distribution. Unfortunately, the DEO is sparingly soluble in aqueous solution at room temperature and is not practical for BTO powder production.<sup>5</sup> Later, present authors employed the thermal decomposition of dimethyl oxalate (DMO) in nitrate ion systems as an alternative to DEO.

In this case, however, the morphology of BTO was found to be multisized instead of being monosized. The final barium titanate (BT) powders were about 3 μm in diameter and consisted of different phases.<sup>6</sup>

In the present study, dimethyl oxalate (DMO) and chloride ions were chosen as an oxalate anion source and as supporting anions respectively. The primary purpose of present study is to investigate systematically the influence of experimental variables such as DMO concentrations, chloride concentrations, temperatures, aging times and etc. on the properties and morphology of the BTO particles produced.

### Experimental

A stock solution of barium chloride was prepared by dissolving the salt of reagent grade (Katayama Chem. Co.) in deionized water to give the nominal barium concentration of 0.2 M. A stock solution of titanium tetrachloride of reagent grade (Yakuri Chem. Co.) was prepared by adding a 160 mL volume of the reagent slowly to a cold distilled water stirred rapidly and diluting to 1 L. The exact titanium

content was determined gravimetrically by the hydroxide precipitation method.<sup>7,8</sup> The final solution was stored in a refrigerator.

Cation stock solutions and the conjugate acidic solutions of supporting anions were added to a beaker in predetermined quantities to adjust the concentration ratio of  $[Ba^{2+}]_0/[Ti^{4+}]_0$  to 1.00 along with a sufficient amount of distilled water to bring the total volume slightly less than 200 mL. The beaker was covered and placed in an isothermal bath that was set at the desired temperature. The predetermined amount of DMO of reagent grade (Katayama Chem. Co.) was added. The solution was brought exactly to 200 mL. The time to onset of precipitation, manifested as the appearance of bluish tint, was recorded for each experiment and adopted as the critical nucleation time.

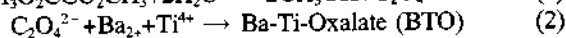
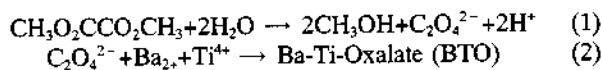
Small aliquots were collected and quenched to 0 °C at regular time intervals to observe development of particle morphologies and growth kinetics. The particles were separated from the supernatant liquid by centrifugation and washed twice with deionized water and twice with ethanol. During the ethanol wash, particles were dispersed with a sonic disruptor. A drop of suspension in ethanol was placed on an aluminium foil and dried for observation of BTO morphology by scanning electron microscope (JEOL JSM 5800 LV).

A 5 mL of precipitated portions settled on the bottom of the beaker were also collected and quenched to 0 °C periodically to observe the overall morphology of the accumulated precipitates at given aging times.

The whole precipitates settled on the bottom of the beaker at given aging times were quenched at 0 °C and were finally separated from the supernatant liquid by centrifugation, dried at 100 °C for 12 h and calcined at 900 °C for 2 h to produce BT powders. Crystallinity and phase purity of the powders were determined by XRD (Rigaku, D/MAS-3C) using Ni-filtered Cu K $\alpha$  radiation.

## Results and Discussion

In the present study, homogeneous precipitation is controlled by the hydrolysis of DMO to generate oxalate anions.



The oxalate concentration at any time  $t$  is a function of the combinations of experimental variables such as the initial concentrations of DMO, concentrations of barium and titanium ions, pH, temperature and concentrations of supporting anions as described previously.<sup>5</sup> This is equivalent to saying that oxalate ion concentration increases with time  $t$  for a given combination of pH, temperature, and initial concentrations of DMO and ions such as  $Ba^{2+}$ ,  $Ti^{4+}$  and supporting anions. And the precipitates will appear at a critical nucleation time  $t_c$ . Since the critical supersaturation value for BTO is observed to be approximately same for all experiments, the reciprocal of the time,  $1/t_c$ , represent a sort of averaged rate of approach to nucleation and is referred to as "rate-to-nucleation (RN)" as described elsewhere.<sup>8</sup>

RN values for various combinations of experimental parameters for chloride solutions at  $([Ba^{2+}]_0 + [Ti^{4+}]_0) = 0.04$  M are given in Table 1. The higher initial concentration of DMO are, the higher values of RN are obtained. These

**Table 1.** Variation of generation rate for oxalate ions with various experimental parameters for chloride system

| Run no. | chloride system    | Temperature (°C) | $\frac{[DMO]_0}{([Ba^{2+}]_0 + [Ti^{4+}]_0)}$ | rate to nucleation ( $min^{-1}$ ) |
|---------|--------------------|------------------|---|-----------------------------------|
| 1       |                    |                  | 2   | 0.01                              |
| 2       |                    | 25               | 4   | 0.10                              |
| 3       |                    |                  | 8   | 0.17                              |
| 4       | $[Cl^-]_0 = 0$     |                  | 2   | 0.16                              |
| 5       | (distilled water)  | 40               | 4   | 0.20                              |
| 6       |                    |                  | 8   | 1.00                              |
| 7       |                    |                  | 2   | 0.24                              |
| 8       |                    | 50               | 4   | 0.50                              |
| 9       |                    |                  | 8   | 1.50                              |
| 10      |                    |                  | 2   | 0.02                              |
| 11      |                    | 25               | 4   | 0.03                              |
| 12      |                    |                  | 8   | 0.05                              |
| 13      | $[Cl^-]_0 = 0.1$ M |                  | 2   | 0.07                              |
| 14      | (0.1 M-HCl)        | 40               | 4   | 0.08                              |
| 15      |                    |                  | 8   | 0.25                              |
| 16      |                    |                  | 2   | 0.33                              |
| 17      |                    | 50               | 4   | 0.33                              |
| 18      |                    |                  | 8   | 0.50                              |
| 19      |                    |                  | 2   | $0.58 \times 10^{-2}$             |
| 20      |                    | 25               | 4   | $1.54 \times 10^{-2}$             |
| 21      |                    |                  | 8   | $1.59 \times 10^{-2}$             |
| 22      |                    |                  | 2   | $1.08 \times 10^{-2}$             |
| 23      | $[Cl^-]_0 = 0.3$ M |                  | 4   | $1.61 \times 10^{-2}$             |
| 24      | (0.3 M-HCl)        | 40               | 8   | $2.48 \times 10^{-2}$             |
| 25      |                    |                  | 2   | $1.54 \times 10^{-2}$             |
| 26      |                    | 50               | 4   | $2.22 \times 10^{-2}$             |
| 27      |                    |                  | 8   | $3.10 \times 10^{-2}$             |

results are similar to those for the formation of ZnS precipitates by homogeneous method.<sup>9</sup>

Table 1 also shows that the higher chloride concentrations are, the slower rates to nucleation are obtained, probably because of formation of more stable species. Below  $RN = 2 \times 10^{-2} min^{-1}$ , it usually took exceedingly long times for precipitation to start (~50 min) and agglomerates of particles were observed especially at relatively higher temperatures and at longer aging times as shown in Table 1 and 2. However, depending on the relative value of RN above  $RN = 2 \times 10^{-2} min^{-1}$  and on aging times, either unimodal, bimodal, or broad unimodal distributions of particle size were observed.

Figure 1 shows a SEM micrograph taken at the aging time of 15–60 min after precipitation had started for run 2 ( $T = 25$  °C,  $([Ba^{2+}]_0 + [Ti^{4+}]_0) = 0.04$  M,  $[Cl^-] = 0.0$  M,  $[DMO]_0 / ([Ba^{2+}]_0 + [Ti^{4+}]_0) = 4$ ) corresponding to a RN value of  $0.10 min^{-1}$ . Here precipitate morphologies were found to be composed of broad unimodal particles of 50–200 nm that were a little fused together, probably because the growth process of particles is predominant. Growth of these particles with aging time is given in Table 2. The bimodal distribution for this run 2 at the longer aging time of 75 min is a result of formation of second generation of particles, as may be observed in the SEM micrograph of Figure 2. The occurrence of bimodal particle morphology at the longer aging time

**Table 2.** Particle Size Distribution with Various Combinations of Experimental Parameters

| Supporting anion  | Temperature (°C) | Concentration $\frac{[DMO]_0}{([Ba^{2+}]_0+[Ti^{4+}]_0)}$ | Aging time                              |   |   |                           |
|---|------------------|---|---|---|---|---------------------------|
|   |                  |   | 15                                      | 30                                      | 60                                      | 90                        |
| [Cl <sup>-</sup> ] <sub>0</sub> =0<br>(distilled water) | 25               | 4   | unimodal<br>and agglomerated<br>~0.2 μm | unimodal<br>and agglomerated<br>~0.2 μm | unimodal<br>and agglomerated<br>~0.2 μm | bimodal<br>1.5 μm, 0.2 μm |
|   | 25               | 2   |   | broad unimodal<br>2 μm, 1.2 μm          | bimodal<br>2.5 μm, 0.8 μm               | bimodal<br>4 μm, 1 μm     |
|   | 25               | 4   | bimodal<br>1.5 μm, 0.5 μm               | bimodal<br>2.2 μm, 1 μm                 | unimodal<br>2.7 μm                      | bimodal<br>3.5 μm, 0.5 μm |
|   | 25               | 8   |   | unimodal<br>3 μm                        | bimodal<br>3.8 μm, 1.2 μm               | bimodal<br>3.8 μm, 1.2 μm |
|   | 40               | 4   |   | unimodal<br>1 μm                        | bimodal<br>1 μm, 0.2 μm                 | unimodal<br>1 μm          |
| [Cl <sup>-</sup> ] <sub>0</sub> =0.1 M<br>(0.1 M-HCl)   | 50               | 4   | unimodal<br>1 μm                        | agglomerated                            | agglomerated                            | agglomerated              |
|   | 25               | 2   |   | bimodal<br>2.7 μm, 0.5 μm               | bimodal<br>2.5 μm, 0.8 μm               | unimodal<br>0.6 μm        |
|   | 25               | 4   | unimodal<br>0.3 μm                      | bimodal<br>2.2 μm, 0.4 μm               | unimodal<br>0.4 μm                      | unimodal<br>0.2 μm        |
|   | 25               | 8   |   | bimodal<br>2 μm, 0.5 μm                 | agglomerated                            | agglomerated              |
|   |                  |   |   |   |   |                           |

suggests that a second generation of particles forms as a direct consequence of growth rate not keeping up with oxalate ion generation. The larger particles (first generation) were found to be formed of dense aggregates of smaller freshly nucleated particles as described elsewhere.<sup>11</sup>

Another perhaps more sensitive parameter on the particle size distribution is the temperature as shown in Table 2. At higher temperature the generation of oxalate ion and the nucleation of precipitates were so rapid that particle size decreased and the degree of agglomeration increased. The particles were agglomerates of smaller particles, and significant necking between particles was observed (not shown). Table 2 also gives the result of particle size distribution measured in chloride supporting anions at various aging times, initial concentrations of DMO and different temperatures. At the ordinary temperature, the change of morphology occurred at

shorter aging time than that at lower temperature even under the condition of lower DMO concentrations. As temperature increased in a given supporting anion, both the nucleation and agglomeration of precipitates were so high that optimization of particle size was difficult.

A further study for aging times was carried out in 0.1 M HCl solution under the condition of temperature of 40 °C and  $[DMO]_0/([Ba^{2+}]_0+[Ti^{4+}]_0)=4$ . The micrographs of BTO particles at various aging times are shown in Figure 3. When the aging time was 15 min, the particles were unimodal as shown in Figure 3(a). At aging time of 30 min, the change to bimodal morphology have occurred as shown in Figure 3(b). At the aging time longer than 60 min, an agglomeration of monosized and spherical particles was observed (Figure 3(c)).

In order to find a possibility for the preparation of BT

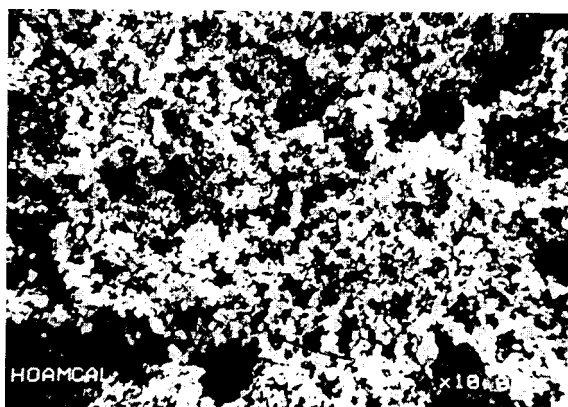


**Figure 1.** A micrograph of the precipitate obtained in distilled water solution with aging time of 15-60 min at temperature of 25 °C and  $[DMO]_0/([Ba^{2+}]_0+[Ti^{4+}]_0)$  of 4.

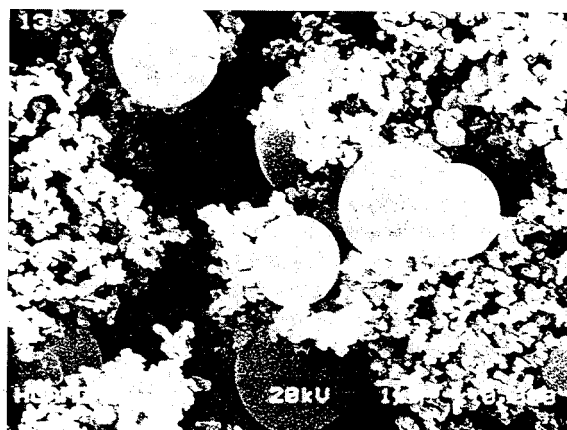


**Figure 2.** A micrograph of the precipitate obtained in distilled water solution with aging time of 75 min at temperature of 25 °C and  $[DMO]_0/([Ba^{2+}]_0+[Ti^{4+}]_0)$  of 4.

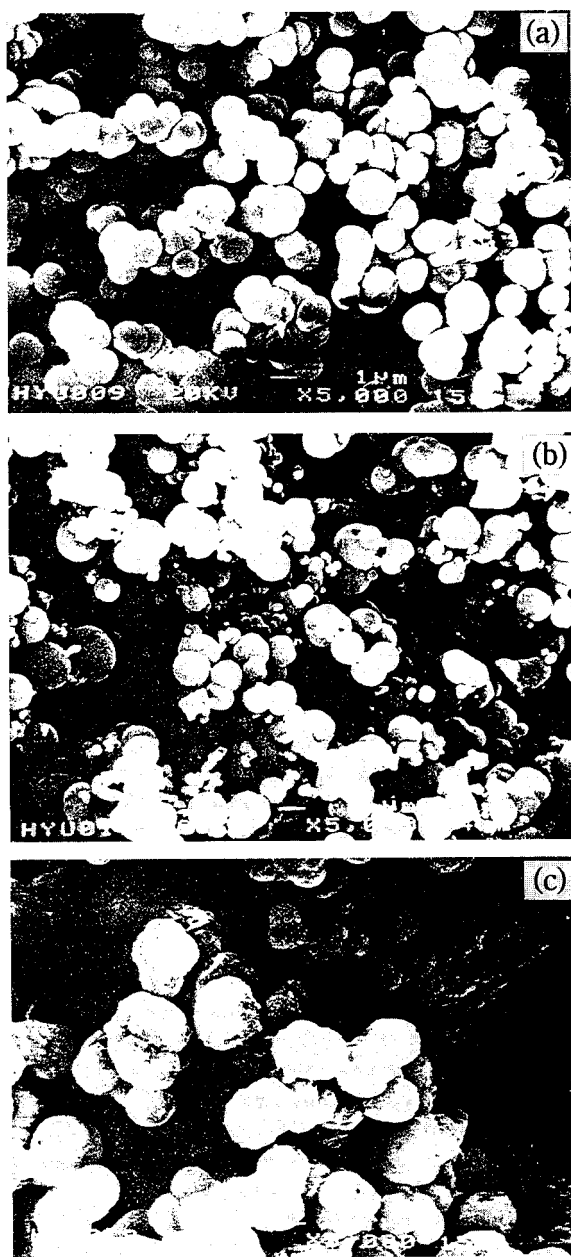


**Figure 3.** Micrographs of precipitate obtained at temperature of 40 °C and  $[\text{DMO}]_0/([\text{Ba}^{2+}]_0 + [\text{Ti}^{4+}]_0)$  of 4 in 0.1 M hydrochloric acid solution with aging time of (a) 15 min, (b) 30 min, (c) 60 min.

powders, the whole unimodal precipitates given in Figure 3(a), settled for 15 min on the bottom of the beaker after the nucleation had started, were collected and treated as described above under "Experimental Procedure". A SEM morphology and a XRD patterns of BT powders thus obtained are given in Figure 4 and 5, respectively. These results give the possibility for the preparation of BT powders with monosized particle distribution and high qualities.

### Conclusion

Particle morphology of BTO was influenced by chloride ion concentrations as well as other experimental variables such as aging times, temperatures and  $[\text{DMO}]_0/([\text{Ba}^{2+}]_0 +$

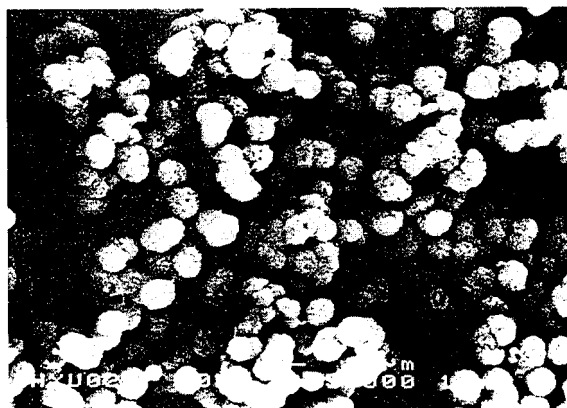


**Figure 4.** A micrograph of calcined BT prepared from BTO which obtained at temperature of 40 °C and  $[\text{DMO}]_0/([\text{Ba}^{2+}]_0 + [\text{Ti}^{4+}]_0)$  of 4 in 0.1 M hydrochloric acid solution with aging time of 15 min.

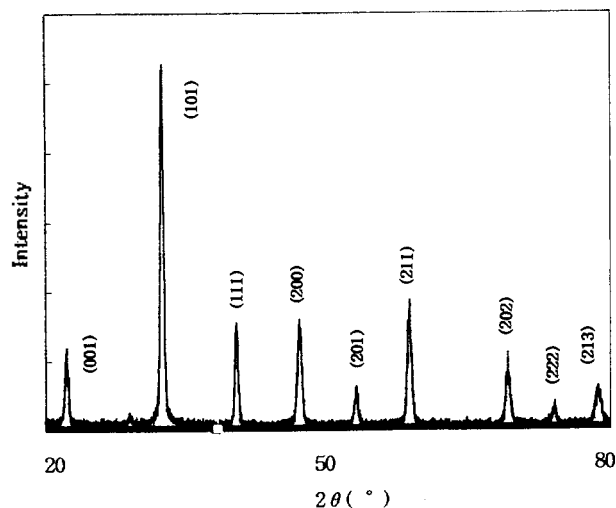


**Figure 5.** A XRD pattern of BT prepared from BTO which obtained at temperature of 40 °C and  $[\text{DMO}]_0/([\text{Ba}^{2+}]_0 + [\text{Ti}^{4+}]_0)$  of 4 in 0.1 M hydrochloric acid solution with aging time of 15 min.

$[\text{Ti}^{4+}]_0$ ). At the very low chloride concentration, relatively smaller particles of BTO about 0.1 μm in diameter were produced. Whereas, at higher chloride concentrations the faster nucleation for precipitation was found with higher temperature and with the higher ratio of  $[\text{DMO}]_0/([\text{Ba}^{2+}]_0 + [\text{Ti}^{4+}]_0)$ , corresponding to the faster transformation of relatively larger particles 0.5~2.5 μm in diameter from unimodal to bimodal or to broad unimodal. BT powders obtained from accumulated precipitates at 0.1 M HCl for 15 min of aging time demonstrated a possible synthesis of monosized BT powders with high qualities.

**Acknowledgment.** The present studies were supported by Basic Science Research Institute Program, Ministry of Education, 1997. Project No. BSRI-97-3439

### References

1. Klee, M. *J. Mater. Sci. Lett.* **1989**, *8*, 985.
2. Moulson, A. J.; Herbert, J. M. *Electroceramics*; Chapman & Hall: London, **1997**, 147.

3. Barringer, E.; Jubb, N.; Fegley, B.; Pober, R. L.; Bowen, H. K. *Processing Monosized Powders*, Ch. 26 in *Ultrastructure Processing of Ceramics, Glasses and Composites*, Edited by Hench and Ulrich, Wiley: New York, 1984, 315.
4. Kim, S.; Lee, M.; Noh, T.; Lee, C. *J. Mater. Sci.* 1996, 31, 3643.
5. Min, C.; Kim, S.; Lee, C. *Bull. Korean Chem. Soc.* 1997, 18, 600.
6. Min, C.; Lee, C. *Anal. Sci. & Technology* 1997, 10, 203.
7. Furman, N. H. *Standard Methods of Chem. Analysis*; Van Nostrand: Princeton, 1962.
8. Noh, T.; Kim, S.; Lee, C. *Bull. Korean Chem. Soc.* 1995, 16, 1180.
9. Celikkaya, A.; Akinc, M. *J. Am. Ceram. Soc.* 1990, 73, 245.
10. *Idem, ibid.* 1990, 73, 2360.
11. Look, J-L.; Zukoski, C. F. *J. Am. Ceram. Soc.* 1995, 78, 21.

## Synthesis and X-Ray Crystal Structure of $[(\eta^5\text{-Tellurophene})\text{Ru}(\eta^5\text{-C}_5\text{Me}_5)](\text{OTf})$

Eui-Hyun Ryu, Hong-Young Chang, and Moon-Gun Choi\*

*Department of Chemistry, Yonsei University, 134 Shinchon-dong, Seoul 120-749, Korea*

*Received March 17, 1998*

In recent years, the coordination chemistry of the group 16 heterocycle ligands of furan, thiophene, selenophene, and tellurophene opens up new research area.<sup>1</sup> Especially the chemistry of thiophene transition metal complexes has been extensively studied<sup>2</sup> as models for industrially and environmentally important hydrodesulfurization (HDS) of sulfur compounds found in crude oil. Among organic sulfur compounds, aromatic thiophene derivatives are the most difficult to desulfurize. This has led to many model studies of the reactions of thiophene and its derivatives with heterogeneous and homogenous systems. The first concern for the HDS catalysis is the binding mode of the thiophene to the catalyst. Three types of coordination modes of the group 16 heterocyclic five membered ligands are most commonly proposed: via the hetero-atom only, as an  $\eta^2$ -coordination involving the unsaturated carbons, or the entire  $\pi$ -system in an  $\eta^5$ -fashion. The need for developing more efficient HDS catalysts requires some novel approaches to obtaining new mechanistic information. One approach is the use of aromatic chalcogen complexes as substitutes for thiophene molecules. The other interest is to investigate the similarity and dissimilarity between the chemistry of thiophene and tellurophene transition metal complexes. Tellurium is an attractive sulfur analogue because of its NMR spectroscopic properties. <sup>125</sup>Te has a 7.03% natural abundance and a nuclear spin of 1/2.<sup>3</sup> The existence of the NMR-active isotope <sup>125</sup>Te makes possible to assign tellurophene bonding modes to the transition metals. The tellurophene is able to coordinate metals through the entire  $\pi$  system as  $\eta^5$  bonding mode. In this paper, the synthesis of  $\eta^5$ -tellurophene coordinated Ru complex and NMR studies of this bonding mode have been reported. In addition, the first X-ray structural determined  $\eta^5$ -coordination mode of tellurophene has been reported.

### Experimental

**General Procedures.** All reactions were performed

under Ar atmosphere in reagent grade solvents, using standard Schlenk techniques.<sup>4</sup> Diethyl ether (Et<sub>2</sub>O) was distilled from Na/benzophenone, CH<sub>2</sub>Cl<sub>2</sub>, and acetonitrile (CH<sub>3</sub>CN) from CaH<sub>2</sub>. MeOH was distilled from Mg. The solvents were stored over 4-Å molecular sieves under Ar. The <sup>1</sup>H and <sup>13</sup>C NMR spectra obtained on Bruker DPX-250 spectrometer with CDCl<sub>3</sub> as the internal lock. The <sup>125</sup>Te NMR spectrum was recorded on the Bruker BZH-300 spectrometer at room temperature and referenced to tellurophene ( $\delta=782$  ppm). Microanalysis was performed with a Perkin Elmer 240 elemental analyzer. Fast atom bombardment (FAB) spectrum was obtained with use of a VG70-VSEQ mass spectrometer.

The following compounds are prepared by literature methods: [Cp\*<sub>3</sub>Ru(CH<sub>3</sub>CN)](OTf)(Cp\*<sub>2</sub>=C<sub>5</sub>Me<sub>5</sub>, OTf=O<sub>3</sub>SCF<sub>3</sub>),<sup>5</sup> Na<sub>2</sub>Te.<sup>6</sup> All other compounds were purchased from commercial sources and used as received.

**Synthesis of tellurophene (1).** Compound 1 was prepared by a modified literature methods.<sup>6,7</sup> To a degassed 5 N sodium hydroxide solution (80 mL) was added Rongalite (sodium formaldehydesulfoxylate dihydrate; HOCH<sub>2</sub>SO<sub>2</sub>Na·2H<sub>2</sub>O, 26.6 g, 0.17 mol) and tellurium (10 g, 78.4 mmol). The solution was refluxed for 2 h under Ar atmosphere. The sodium telluride as a wine-colored solution was formed. After the solution was evaporated under vacuum, the yellowish white sodium telluride was obtained. This sodium telluride is very air sensitive. To the yellowish white powder, dry degassed methanol (160 mL) was added and the mixture was stirred until the solid dissolved (system A). The butadiyne was prepared separately in a three-neck flask a gas inlet, and a condenser connected through a trap to a column (40×2.5 cm) filled with anhydrous calcium chloride and outlet needle. To a degassed solution of potassium hydroxide (5 N, 150 mL) was added 1,4-dichloro-2-butyne (25.2 g, 205 mmol) in dioxane (20 mL) (system B). Systems A and B were connected and flushed with a slow stream of dried Ar. The solution in system B was heated under reflux with vigorous stirring and the butadiyne was